

Article

Investigation of Individual Cells Replacement Concept in Lithium-Ion Battery Packs with Analysis on Economic Feasibility and Pack Design Requirements

Manh-Kien Tran ^{1,*}, Carlo Cunanan ¹, Satyam Panchal ², Roydon Fraser ² and Michael Fowler ¹

¹ Department of Chemical Engineering, University of Waterloo, 200 University Avenue West, Waterloo, ON N2L 3G1, Canada; cjcunanan@uwaterloo.ca (C.C.); mfowler@uwaterloo.ca (M.F.)

² Department of Mechanical and Mechatronics Engineering, University of Waterloo, 200 University Avenue West, Waterloo, ON N2L 3G1, Canada; satyam.panchal@uwaterloo.ca (S.P.); rafraser@uwaterloo.ca (R.F.)

* Correspondence: kmtran@uwaterloo.ca; Tel.: +1-519-888-4567 (ext. 33415)

Abstract: The optimization of lithium-ion (Li-ion) battery pack usage has become essential due to the increasing demand for Li-ion batteries. Since degradation in Li-ion batteries is inevitable, there has been some effort recently on research to maximize the utilization of Li-ion battery cells in the pack. Some promising concepts include reconfigurable battery packs and cell replacement to limit the negative impact of early-degraded cells on the entire pack. This paper used a simulation framework, based on a cell voltage model and a degradation model, to study the feasibility and benefits of the cell replacement concept. The simulation conducted in MATLAB involves generating and varying Li-ion cells in the packs stochastically and simulating the life of the cells as well as the packs until they reach their end-of-life stage. It was found that the cell replacement method can increase the total number of cycles of the battery packs, effectively prolonging the lifespan of the packs. It is also determined that this approach can be more economically beneficial than the current approach of simple pack replacement. For the cell replacement concept to be practical, two main design criteria should be satisfied including individual cell monitoring and easy accessibility to cells at failure stage.

Keywords: lithium-ion battery; battery cell replacement; battery modeling; battery degradation; battery cost analysis; battery life optimization



Citation: Tran, M.-K.; Cunanan, C.; Panchal, S.; Fraser, R.; Fowler, M. Investigation of Individual Cells Replacement Concept in Lithium-Ion Battery Packs with Analysis on Economic Feasibility and Pack Design Requirements. *Processes* **2021**, *9*, 2263. <https://doi.org/10.3390/pr9122263>

Academic Editors: Andrey Voshkin and Antonio Bertei

Received: 3 November 2021

Accepted: 15 December 2021

Published: 16 December 2021

Publisher's Note: MDPI stays neutral with regard to jurisdictional claims in published maps and institutional affiliations.



Copyright: © 2021 by the authors. Licensee MDPI, Basel, Switzerland. This article is an open access article distributed under the terms and conditions of the Creative Commons Attribution (CC BY) license (<https://creativecommons.org/licenses/by/4.0/>).

1. Introduction

Renewable energy sources play an important role in providing sustainable and clean energy and mitigating climate change globally [1]. The development of renewable energy harvestings such as solar and wind has raised the demand for energy storage systems and transportation methods with reduced CO₂ emissions [2]. Energy storage systems are the key to enabling the storage and dispatch of electricity from renewable sources [3]. Lithium-ion (Li-ion) batteries, as an energy storage system, have gained in popularity in recent years, especially in automotive applications and large-scale energy storage facilities due to their high energy and power density, long cycle life, high fidelity with high temperature tolerance, low self-discharge rate, and rapid charging capabilities [4–6].

Li-ion battery cells can degrade through cycles of discharge and charge as well as over time even when they are inactive, with dependency on both temperature and state of charge (SOC) [7,8]. The degradation that occurs through discharge and charge is called cycling aging, while degradation that happens when it is not in use is called calendar aging [9]. The degradation in Li-ion batteries reduces the amount of energy and power that could be delivered in battery applications. After a certain number of cycles, Li-ion cells will eventually reach their end-of-life (EOL) stage. In some applications such as electric vehicles the EOL threshold of a battery is often when its remaining total capacity reaches 80% of its initial total capacity [10].

As battery packs consist of multiple cells, the potential and performance of the pack would be an overall average reflection to the state of each cell, but not specific to any certain cell [11]. Often in reality, due to the variability in characteristics of the cells, not all cells behave and degrade at the same rate [12]. Factors such as the pack's thermal management, SOC inhomogeneities, and manufacturing configurations are some of the reasons leading to the variation of the capacity fade of individual cells in the same pack [13]. As the battery pack reaches its EOL stage, it would likely contain some cells that are in a healthier state than other cells [14]. This makes replacing the entire pack not completely efficient since some of the cells would still be in usable conditions. The discarding of usable cells would effectively lead to unnecessary costs in Li-ion battery energy storage systems [15,16]. An alternative strategy would be making the battery pack reconfigurable for individual cell replacement, so that only less healthy cells would be replaced with newer cells, instead of replacing the entire battery pack [17]. This strategy involves monitoring the levels of capacity fade of each individual cell and swapping out the most degraded cells based on a pre-specified capacity fade threshold. As a result, the effect of imbalance and premature aging in the pack could be minimized, and the degraded cells can be eliminated before causing more damage to the pack.

Some studies have been previously conducted to investigate the cell replacement concept. Kampker et al. [18] proposed a battery remanufacturing framework and suggested that the optimal depth of disassembly was up to the cell level, based on the reliability characteristic and the architecture of the cells within the battery applications. Mathew et al. [19] provided further analysis to a Li-ion cell replacement framework with data collected from the simulation to examine the optimal cell replacement interval. Nenadic et al. [20] examined the most viable cell replacement strategies under two scenarios of the pack's early-life failure and reuse of Li-ion battery packs in less demanding applications. Some other recent studies have also explored cell-to-cell variation, which could further prove the effectiveness of the cell replacement concept. Lu et al. [21] proposed a method to evaluate cell-to-cell variation in Li-ion batteries based on five cloud indicators during charging. Omariba et al. [22] showed various Li-ion cell balancing methodologies to mitigate cell-to-cell variation and evaluate its relationship with the overall battery performance. As individual cell aging has an undermining effect on the lifespan of a battery pack, Rehman et al. [23] proposed a lifespan-extending algorithm that targets individual Li-ion cells differently to reduce any increase in the capacity mismatch. Zheng et al. [24] extended the investigation of the aging effect to a Li-ion battery pack by analyzing the evolution of battery capacity loss using the electric quantity capacity scatter diagram (ECSD) cell aging mechanism.

The concept of cell replacement in Li-ion battery packs is relatively new, and despite some recent efforts to investigate this concept, the feasibility, in terms of economics and design, of cell replacement has not been well-studied. In this paper, a battery voltage model and a battery degradation model are presented to develop a cell replacement simulation framework. The simulation framework was then used to investigate the economic feasibility and design requirements of the cell replacement idea. Specifically, a pack of 40 Li-ion cells was simulated to its EOL stage, and another set of 40 Li-ion cells was used as the replacement for the cells in the original pack. The simulation was conducted repeatedly using MATLAB to determine whether replacing cells individually would be more beneficial in terms of battery life and costs, compared to replacing the entire pack that could still consist of healthy cells. The results of the simulation in this study were then analyzed to decide whether the cell replacement concept would be practical, or under what conditions it would be practical for use in real-world applications. The rest of this paper is organized as follows. Section 2 describes the experimental design and setup used in this study, while Section 3 presents the battery models and the details of the cell replacement simulation framework used in this work. Section 4 provides the results of the simulation and some discussions on the feasibility and benefits of the cell replacement concept. Finally, the resulting conclusions are given in Section 5.

2. Experimental

Lithium iron phosphate (LFP) pouch cells were used in this study. The specifications of the cells are shown in Table 1. The nominal capacity of the cells was 20 Ah, and the rated voltage range was 2.00–3.65 V. Experimental data were necessary to develop a realistic and robust battery cell model for the simulation. The mean and variance of the parameter values gathered in these experiments were used to generate randomized parameter values in the simulation. Specifically, the data were obtained by performing tests on four different LFP cells. The mean and variation in the parameters experimentally were then used to develop a distribution that was applied to stochastically generate the parameters for the 10 sets of 80 cells in the simulation framework, which will be further explained in Section 3.

Table 1. Lithium-ion pouch cell specifications.

Specifications	Value
Nominal Capacity	20.0 Ah
Nominal Voltage	3.3 V
Voltage Limits	2.0–3.65 V
Cell Weight	496 g
Dimensions	7.25 mm × 160 mm × 227 mm
Operating Temperature	−30–55 °C

The experiments were all conducted using a MACCOR 4200 battery cycler. The experimental setup is shown in Figure 1. The two types of experimental procedures conducted to obtain the data were a hybrid pulse power characterization (HPPC) test and the determination of the open-circuit voltage (OCV) to produce the SOC–OCV curve. The HPPC test is often used to determine the dynamic power capability over a useable voltage range of a given cell or battery [25]. In this study, the HPPC tests were used to determine the ohmic resistance and the polarization resistance and capacitance of the cells as a function of the SOC. The determination of the SOC–OCV curve is useful to estimate the OCV as a function of the SOC, which can be used in further equations in the equivalent circuit model (ECM).



Figure 1. Experimental setup: experimental setup and MACCOR 4200 battery cycler (left); and tested 20 Ah battery pouch cells (right).

First, the HPPC test was used to determine the parameters for the ECM (R_0 , R_1 , C_1) at each SOC from 20% to 90%. To start, the cell was charged or discharged to the desired starting SOC of either 20% or 90%. The HPPC test was then carried out for both charging and discharging at 10% intervals between 20% and 90% SOC. The HPPC pulse consisted of

a 1 C discharge for 10 s, a 40-s rest period, and a 0.75 C charge for 10 s. To move between the 10% SOC intervals, a constant-current discharge or charge of 1 C of 6 min and a subsequent rest for 1 h was performed. Second, the OCV curves were determined for the four cells across the SOC range of 0% to 100%, and the final curve was taken as the average of the four curves. For this test, the cells, at full charge, were subjected to a C/25 discharge current until they were completely drained, followed by an hour of rest, and then a C/25 charge until they were fully charged. The overall OCV curves were determined by taking the average of the charge and the discharge curves.

3. Modeling and Simulation

3.1. Cell Voltage Model

3.1.1. Model Development

The battery cell voltage model used to represent the cells in this study was the Thevenin ECM, as shown in Figure 2. This model provides a good balance between computational efficiency and accuracy [26–29]. The Thevenin ECM consists of four main parameters, which are V_{oc} , R_0 , R_1 , and C_1 . V_{oc} represents the OCV of the battery; R_0 represents the internal resistance of the cell; and R_1 and C_1 represent the transient behavior of the cell as an RC pair with one being a resistor and the other being a capacitor. R_1 and C_1 are in parallel with each other, but in series with the voltage source and the R_0 element.

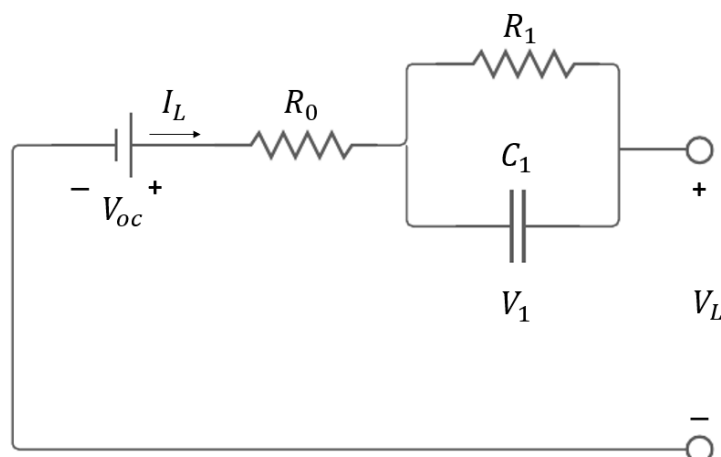


Figure 2. Schematic of the Thevenin equivalent circuit model.

The equations for the Thevenin ECM are shown below:

$$\frac{d(V_1)}{dt} = \frac{V_1}{R_1 C_1} + \frac{I_L}{C_1} \quad (1)$$

$$V_L = V_{oc} - V_1 - I_L R_0 \quad (2)$$

Using the OCV test and the HPPC test, the values of the four parameters (V_{oc} , R_0 , R_1 , and C_1) can be obtained at different SOC levels. The current I_L is an input variable to the model. The terminal voltage V_L can then be determined by solving Equations (1) and (2).

3.1.2. Model Validation and Results

The overall OCV curve was determined by averaging the four individual cell curves obtained from the OCV tests. The resulting final curve is shown in Figure 3. Following the HPPC procedure, the other three ECM parameters (R_0 , R_1 , and C_1) were determined at the SOC levels between 20% and 90%. The results are plotted in Figure 4. For the overall trends, it can be seen that as SOC increased, the R_0 value decreased, the R_1 value stayed the same, and the C_1 value increased. However, since the values of the ECM parameters were close enough along the SOC range to be used in the cycling simulation, they will be assumed as lookup tables—and not a continuous function of the SOC—when they are generated.

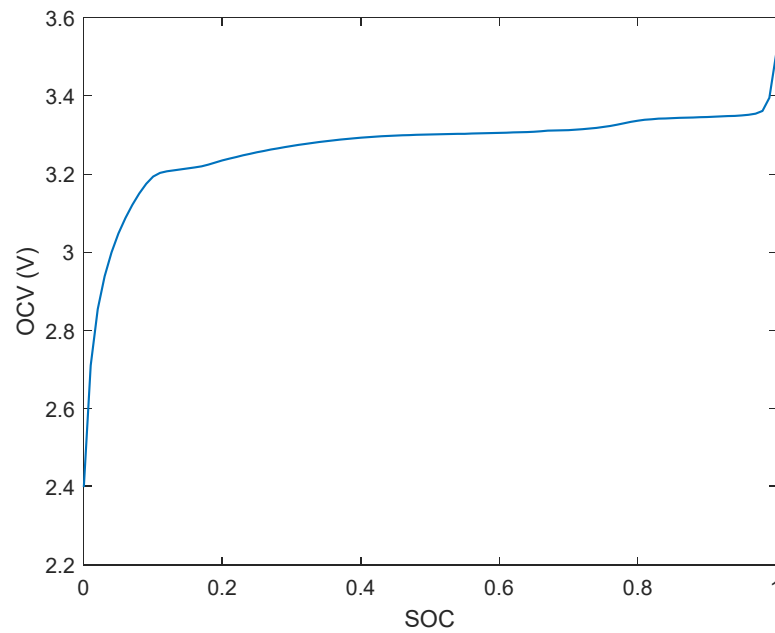


Figure 3. Experimentally established SOC–OCV curve of the LFP cells.

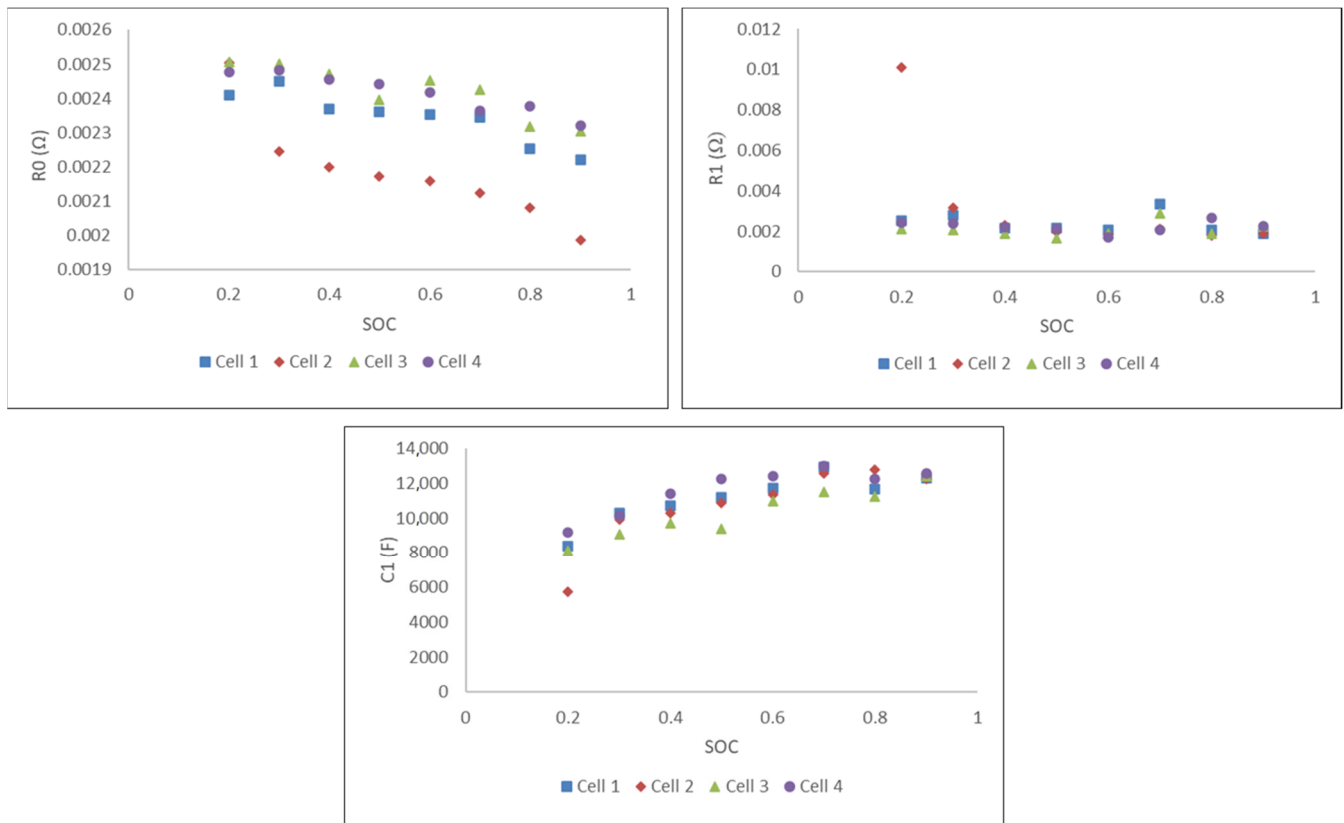


Figure 4. ECM parameters obtained from the HPPC tests: R_0 (top left), R_1 (top right), and C_1 (bottom).

To validate that the cell voltage model is viable, the Urban Dynamometer Driving Schedule (UDDS) was used. The UDDS cycle is commonly used to replicate the driving conditions within a city. The current profile from the UDDS was tested experimentally on the battery, and the corresponding experimental voltage values were measured. Then, the voltage values predicted from the ECM with the current profile input and the newly obtained parameters were compared to the measured values, as seen in Figure 5. It was

seen that the model was well-fitted to the experimental data, with an average absolute percent error of around 0.6%.

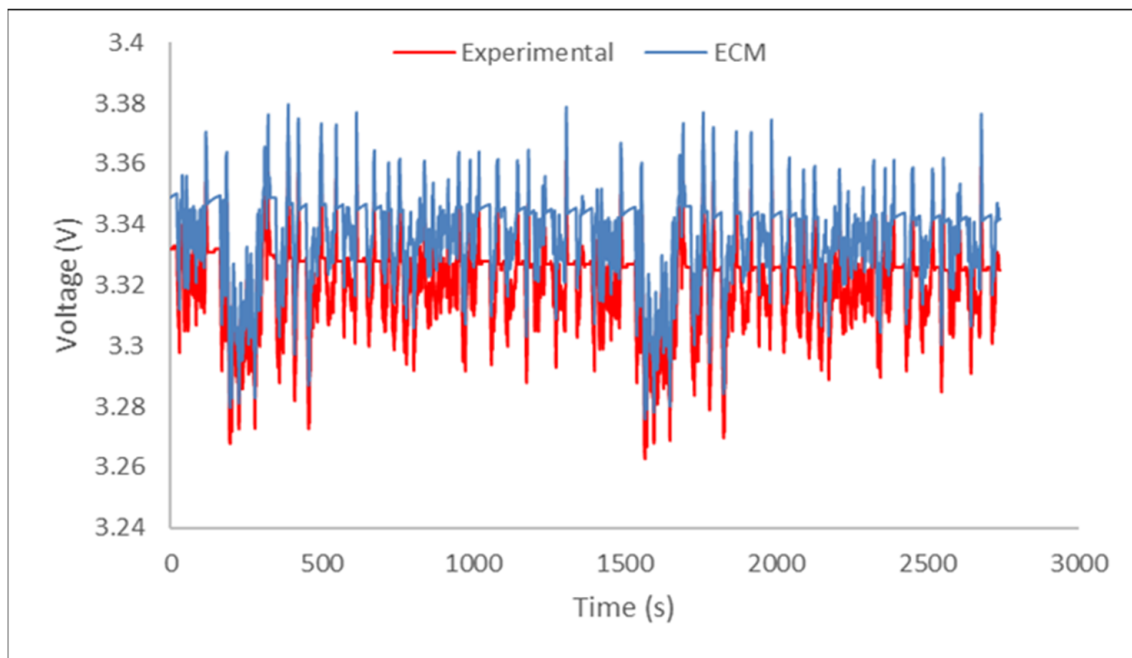


Figure 5. Cell voltage model validation plot using UDDS cycle.

For the equations used in the simulation framework, shown in later sections, the mean and the standard deviation values were utilized to establish the distribution of the parameters. These would be the X_{mean} and the $Stdev$ in Equation (6). The mean of the parameter values between the four cells was taken at 50% SOC. The standard deviation of the capacity and the R_0 parameter was around 2–5%, while the R_1 and C_1 parameters had a standard deviation of 10–12% between the four cells. The results are displayed in Table 2, and these values were subsequently used in the simulation in Section 3.4, specifically in Equation (6).

Table 2. Capacity and ECM parameters distribution.

Parameter	Mean	Standard Deviation	Units
Capacity	19.1750	0.4787	Ah
R_0	0.0023	0.00012	Ω
R_1	0.0019	0.00023	Ω
C_1	10921	1188.1	F

3.2. Cell Degradation Model

There are several methods to quantify and simulate battery cell degradation [30–32]. The battery degradation model used in this analysis was based on the empirical model proposed by Schmalsteig et al. [32]. This battery degradation model was used and validated in our previous work [19]. This model was chosen because it is empirical, which would require less computational time, and because it has fitting parameters that could vary stochastically, which allows for more realistic cell variation. This degradation model takes into consideration the effects of the depth of discharge (DoD) and the average voltage (V_{avg}) of the cell throughout the current profile. This was simplified to depend only on cycling aging and neglect calendar aging for the purpose of this study. The degradation model was coupled with the voltage model to predict the degradation profile of the cells.

The degradation model used in the simulation framework involves Equations (3)–(5). CAP_{cyc} represents the ratio between the current total cell capacity and the initial total cell

capacity, which indicates capacity fade. This value decreases as cycling progresses. Res_{cyc} represents the ratio between the current cell resistance to the initial cell resistance. This value increases as cycling progresses. $Q_{processed}$ represents the charge throughput. The $\beta_{cap/res}$ represents β_{cap} or β_{res} , which are the parameters for capacity fade and resistance increase in Equations (3) and (4). Both were calculated using the same equation but with different values of a , b , c , and d , which are shown in Section 3.4.

$$CAP_{cyc} = 1 - \beta_{cap} \sqrt{Q_{processed}} \quad (3)$$

$$Res_{cyc} = 1 + \beta_{res} Q_{processed} \quad (4)$$

$$\beta_{cap/res} = a(V_{avg} - b)^2 + c + d(DoD) \quad (5)$$

3.3. Pack Voltage Model

The pack voltage model was used to combine the individual cell voltage models in series to obtain the overall performance of the battery pack by simplifying n Thevenin ECMs in series into a single Thevenin ECM with n RC circuits. This model was used to produce the pack voltage, OCV, and SOC corresponding to the current profile and determine the pack capacity. The information obtained can be used to evaluate the overall performance of the pack as it degrades. The pack voltage model was also used to update the cell-level ECM parameters to make sure that all cells were realistically subjected to the same current profile as they were connected in series. However, the variation in individual cell degradation rates can lead to variance in some cycling characteristics such as DoD and SOC.

3.4. Cell Replacement Simulation Framework

The simulation in this study was performed using object-oriented programming in MATLAB. It utilized the three different models described in previous sections: the cell voltage model, the cell degradation model, and the pack voltage model. Figure 6 outlines the overall simulation framework.

The simulation initially generated 10 sets of 80 individual LFP cells, which were all stochastically vary in their capacity, ECM parameters, and degradation parameters. The ECM parameters (R_0 , R_1 , C_1) and the capacity were generated for each cell using Equation (6),

$$Y = X_{mean} + X_{mean}(Rand)(Stdev) \quad (6)$$

where Y represents the parameter values generated for an individual cell; X_{mean} is the average of the given parameter across the four cells from the experiment; $Rand$ is a normally distributed random number between -1 and 1 ; and $Stdev$ is the standard deviation of the given parameter across the four cells from the experiment.

The degradation parameters for each cell in the simulation were generated using the formula below:

$$Y = Z + Z(Var)(Rand) \quad (7)$$

where Y represents the values of the generated parameter, while Z is the degradation parameter values given in Table 3 that were taken from our previous work [19]. Var is the variability of the model, which was 3% in this study. However, for parameter b , the Var value was further divided by 2. $Rand$ is a normally distributed random number between -1 and 1 .

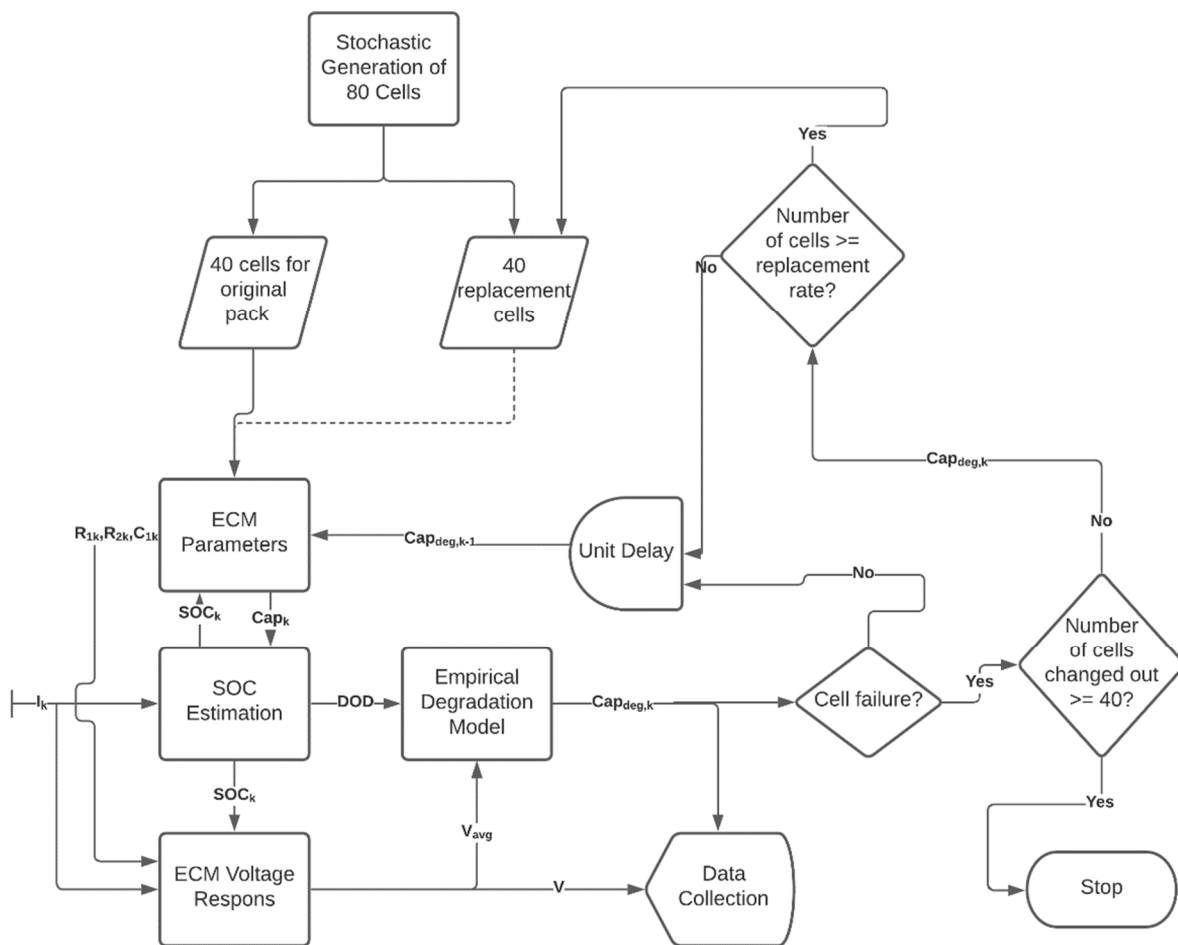


Figure 6. Schematic of the cell replacement simulation framework.

Table 3. Degradation parameters used in the simulation.

Parameter	Capacity Fade	Resistance Rise	Units
<i>a</i>	0.00142	2.780×10^{-5}	$\sqrt{\text{AhV}}^{-1}$
<i>b</i>	3.274	3.199	V
<i>c</i>	0.00119	-2.237×10^{-5}	$\sqrt{\text{Ah}}^{-1}$
<i>d</i>	-9.219×10^{-4}	7.361×10^{-5}	$\sqrt{\text{Ah}}^{-1}$

The stochastic variation techniques described above provided a reasonable estimation of how a real-world pack would degrade over time. For each of the 10 sets of cells, the 80 cells were indexed, and the first 40 cells were used, in series, in the initial battery pack. The 40-cell packs (2.64 kWh) represent standard battery packs used in various real-world applications. The other 40 cells would be used when the cells in the initial pack needed replacement.

The battery packs simulated were subjected to discharge and charge cycles of 1 C between 20% and 80% average SOC. The simulation started at 80% for each cell. One cycle refers to one complete discharge and charge of a cell. The determination of the current amount needed to achieve 1 C was based on the total capacity of the pack. The SOC of each cell was determined using Equation (8), which is based on the coulomb counting method [33], where I is the battery current, SOC_0 is the initial SOC, and C_n is the maximum battery capacity.

$$\text{SOC} = \text{SOC}_0 + \frac{1}{C_n} \int \frac{I}{3600} dt \quad (8)$$

The voltage was determined using the ECM model for each cycle. The voltage and the SOC values were then used in the degradation model to calculate the capacity fade. The capacity of each cell was checked each cycle to ensure that the cells were below the cell failure limit.

A maintenance event is defined as the time at which at least one cell replacement occurs. The replacement rate is defined by the number of cells that have gone below the cell failure limit and would be replaced during a maintenance event. The cell failure limit for the main case study was 82% state of health (SOH) or CAP_{cyc} . For example, if the replacement rate is 4, then four individual cells would have to fall below 82% SOH before a replacement (maintenance event) would occur. The replacement would immediately swap the four old cells with four fresh cells from the remaining 40 fresh cells that were not initially put into the pack. This would result in 10 maintenance events in the simulation as there are 40 other cells. The replacement would also rely on the indices of the cells, occurring in order from cell 41 to cell 80. The four fresh cells for the first maintenance event in this example would be the cells indexed from 41 to 44. The replacement rates tested in this study were for every 1, 2, 4, 5, 8, 10, and 20 cells. The values of replacement rates were selected as there were 40 additional cells, and in order to utilize all the additional cells, the rates need to be divisors of 40. In addition there was a simulation for simply an ordinary pack replacement (no cell replacement), which acted as a reference point for comparison between cell replacement and no cell replacement. In the pack replacement case, the initial pack would be replaced with a new pack consisting of the remaining 40 cells, with completely new packaging as there would be no cell replacement when the pack's SOH has fallen below 80%.

The cell failure limit was chosen to be higher than the pack failure limit of 80% as it was necessary for the cell failure limit to be above the pack failure limit to ensure that most cells did not degrade past 80%. However, if the cell failure limit was set too high, then there would be cells that are replaced while still being relatively healthy. Therefore, in the main case study, it was determined to be 82%. An additional test was performed with a cell failure limit of 72% and a pack failure limit of 70%.

The capacity of each cell was recorded for each cycle. The pack capacity was calculated based on the capacity of the weakest cell. The SOH of the pack is the ratio between the weakest cell capacity and the nominal cell capacity, given by the equation

$$SOH_{pack} = \frac{\min(Cap_{cell1}, Cap_{cell2}, \dots, Cap_{cellN})}{Nominal\ Cell\ Capacity} \times 100 \quad (9)$$

4. Results and Discussion

4.1. Cell Replacement Concept Simulation and Results

The simulation across the 10 datasets of 80 cells showed that the total number of cycles in the lifespan of a battery pack generally increases when the replacement rate increases. It should be noted that when the replacement rate increases, the number of maintenance events decreases because the greater number of cells replaced at each maintenance event would result in fewer maintenance events. Figure 7 shows the results of the cell replacement simulation with different replacement rates, for the battery pack's SOH thresholds of 80% (cell's SOH threshold of 82%) and 70% (cell's SOH threshold of 72%). The total number of cycles was calculated as the average of the 10 sets of 80 cells that were simulated, with each set yielding a battery pack of 40 cells as well as 40 additional replacement cells.

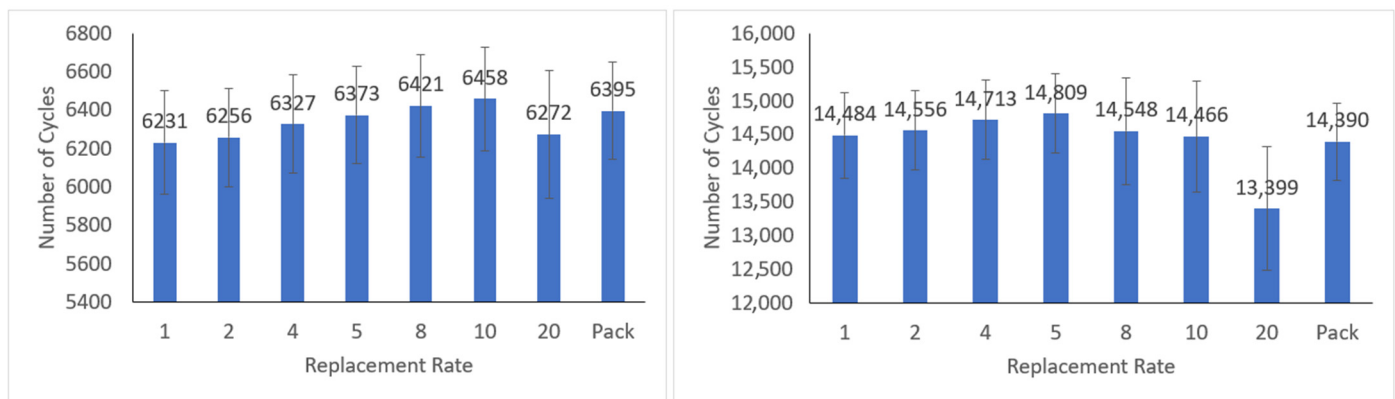


Figure 7. Total number of cycles, on average, of the battery packs with different replacement rates, for 80% SOH threshold (left), and 70% SOH threshold (right).

From Figure 7, for the pack SOH threshold of 80%, it was observed that a replacement rate of 10 (replacing 10 cells at every maintenance event) allowed for the greatest number of cycles, which was 6458 cycles. An ordinary pack replacement, which is the common practice currently, gave a total number of 6395 cycles, which was 63 cycles lower than the case with the replacement rate of 10. However, the replacement rate of 10 would require four maintenance events, meaning an additional three visits to the vehicle shop or dealership compared to the pack replacement method. The pack replacement approach was also shown to have better results than most other cell replacement cases, except for cases with replacement rates of eight and 10. The lowest number of cycles was given by the replacement at every 20 failed cells, which was 6272 cycles. This is likely because the SOH of the pack fell below 80% before its 20 individual cells broke down below 82%.

Figure 7 also indicates that lowering the threshold from 80% SOH to 70% SOH with a cell failure limit of 72% led to an increase, by over double in all cases, of the total number of cycles. The average total number of cycles for the optimal replacement rate was 14,809 cycles for the replacement rate of five. This was 8351 cycles more than the case of the 80% SOH threshold. The pack replacement approach, in this case, resulted in an average of 14,390 cycles, which was 419 fewer cycles than the best cell replacement case, or around 3% lower instead of only 1% such as in the 80% SOH threshold case. The pack replacement method also then gave worse results than most other cell replacement cases except for the case with the replacement rates of 20. This indicated that lowering the pack SOH threshold could provide a significantly greater battery life if lower battery capacity was acceptable to the application, which is the case for many stationary battery applications. It was noted that if continuous cell replacement is performed, then there will be cases where a lot of replacements occur at times close to each other, especially for low replacement rates such as 1, 2, or 4. This might prove inconvenient in the real-world setting when several replacements might occur on the same day or week.

4.2. Battery Pack Design Requirements for Cell Replacement Concept

For the cell replacement concept to be feasible in the real-world setting, there are two main design criteria to be considered. The two criteria include good individual cell monitoring and identification and easy accessibility to the cells that need replacement. The first criterium is achieved when a battery management system (BMS) is installed so that one can monitor each cell's SOH. This design consideration is indispensable in the future for the BMS, not only because of cell replacement, but also due to cell aging, balancing, and safety [34]. It also allows for the second criteria to be met since, without individual cell identification, cell replacement cannot be conducted effectively. The second design criterium is achieved if cells can easily be removed and installed physically in the pack. This can be difficult at the moment as many battery packs nowadays use fusion to connect cells together [35,36]. Fusion is the act of using molten metals similar in composition to

the current-carrying parts to create an electrical pathway for the cells to be placed in series or parallel. This is seen as the most advanced and reliable approach because it creates less interfacial resistance problems, which can often occur in other methods of connecting cells such as through simple physical contact of the current-carrying parts. This design consideration is required for the cell replacement concept to be practical, as it would not be economical to spend a significant amount of time and labor to replace individual cells in the battery pack. This criterion can be achieved if one can find a way to make compression—physical contact—a viable option for internal cell connections or a way to easily replace cells that are fused within a battery pack.

4.3. Economic Feasibility of Cell Replacement Concept

The economic benefit and feasibility of the cell replacement concept were assessed by estimating the price of the cases using cell replacement versus pack replacement. The costs were then related to the cycling performance of the packs in both the 70% and 80% SOH threshold cases. This was used to make conclusions on when cell replacement would become beneficial.

First, the cost of each cell was set to \$28, which was the original price of the LFP cells. This was then multiplied by the number of cells and the cells-to-pack cost proportion to obtain the total cost of the original pack as well as the proportion of the cost between the material and the pack. The cells-to-pack cost proportion was set to 48% as Wentker et al. [37] suggested. However, a 50% price increase was added to the manufacturing costs of the packs for the cell replacement cases because it would require a different and robust design and result in greater costs. To obtain the total cost of the pack replacement case, the original pack cost was doubled as one would simply replace the original battery pack with another similar pack with the same price. For the cell replacement cases, only the costs of the cells were considered because a brand-new pack is not necessary with the pack systems that are already in place being reused. Finally, the labor costs were set to \$100 per maintenance event. The number of maintenance events was selected according to the optimal number of cycles for both the 70% and 80% SOH threshold cases, which were eight and four, respectively. A summary of the cost analysis and comparison between cases of pack replacement and cell replacement is shown in Table 4.

Table 4. Cost analysis and comparison between cases of pack replacement and cell replacement.

	Pack Replacement	Cell Replacement
Cell cost (USD/cell)	\$28.00	\$28.00
Total number of cells in one pack	40	40
Cells-to-pack cost proportion	48%	NA
Cell cost for original pack (40 cells)	\$1120.00	\$1120.00
Initial pack manufacturing cost	\$1213.33	\$1820.00
Total cost of original pack	\$2333.33	\$2940.00
Total cost of replacement	\$2333.33	\$1120.00
Total labor cost of replacement (for 80% SOH threshold)	\$100.00	\$400.00
Total labor cost of replacement (for 70% SOH threshold)	\$100.00	\$800.00
Total cost (for 80% SOH threshold)	\$4766.67	\$4460.00
Total cost (for 70% SOH threshold)	\$4766.67	\$4860.00

The results show that the total pack replacement costs were estimated to be around \$4766.67 while the total cell replacement costs were \$4860.00 and \$4460.00 for the 70% and 80% SOH threshold cases, respectively. This indicates that the cell replacement costs were cheaper for the 80% SOH threshold case, but not for the 70% SOH threshold due to the increased number of maintenance events that led to higher total costs. For the 80% SOH threshold case, the total cost of cell replacement was about 6% (or \$306.67) lower than that of pack replacement, while being able to improve the total number of battery

pack cycles by 1% (or 63 cycles). For the 70% SOH threshold case, even though the cell replacement's total cost was about 2% (or \$93.33) higher than the pack replacement's total cost, the cell replacement method was able to increase the total number of pack cycles by 3% (or 419 cycles). In both cases, the cell replacement approach can be seen as a better option than the pack replacement approach. Overall, it can be concluded that if the design requirements for the cell replacement concept are fulfilled as discussed in Section 4.2, this concept will be feasible and beneficial economically.

5. Conclusions

This study investigated the concept of cell replacement for Li-ion battery packs using MATLAB simulation based on experimental data from 20-Ah LFP pouch cells. A battery voltage model and a battery degradation model were used to set up the simulation framework. The simulation stochastically generated 10 sets of runs, with each set consisting of 80 LFP cells where 40 cells were put in a battery pack and the other 40 cells were utilized as additional cells for replacement. The investigated pack failure SOH thresholds were 70% and 80%, while the cell failure SOH thresholds were 72% and 82%, respectively. The main conclusions from this work are as follows:

1. The cell voltage model was validated and can be used to generate cells stochastically.
2. The cell replacement approach can increase the total number of battery cycles by 63 cycles (or a 1% increase), on average, in the 80% SOH threshold case. This approach can also increase the total number of cycles by 419 cycles (or a 3% increase), on average, in the 70% SOH threshold case.
3. Lowering the pack SOH threshold from 80% to 70% would significantly increase the total number of cycles if the battery application could accept the lower battery capacity.
4. The cell replacement concept is only feasible if two main design criteria can be satisfied including individual cell monitoring and identification and accessibility to cells that require replacement. However, these design requirements can be difficult to achieve without significant costs.
5. If the design requirements can be met, the cell replacement method will be more economically beneficial than the current pack replacement approach as it allows the reuse of many different components of the battery pack.

The findings in this study show that the cell replacement concept can be viable and more economically beneficial than the current approach of replacing the entire pack, given that the design requirements are fulfilled. Future research work will focus on other evaluation criteria to highlight the advantages of the cell replacement concept such as supply chain benefits, maintenance ease, waste reduction, etc. as well as other chemistries of Li-ion batteries, the use of better battery models, and the approach to satisfy the design requirements discussed in this paper.

Author Contributions: Conceptualization, M.-K.T. and M.F.; Data curation, C.C.; Formal analysis, M.-K.T. and C.C.; Funding acquisition, M.F.; Investigation, M.-K.T. and C.C.; Methodology, M.-K.T. and M.F.; Project administration, S.P.; Resources, S.P., R.F. and M.F.; Software, M.-K.T. and C.C.; Supervision, R.F. and M.F.; Validation, M.-K.T.; Visualization, M.-K.T.; Writing—original draft, M.-K.T. and C.C.; Writing—review & editing, S.P., R.F. and M.F. All authors have read and agreed to the published version of the manuscript.

Funding: This work was supported by the Department of Chemical Engineering at the University of Waterloo, Canada Research Chair Tier I—Zero-Emission Vehicles and Hydrogen Energy Systems Grant number: 950-232215, and The Natural Sciences and Engineering Research Council of Canada (NSERC), Discovery Grants Program, RGPIN-2020-04149.

Acknowledgments: This work was supported by equipment and manpower from the Department of Chemical Engineering at the University of Waterloo. Special thanks to Ian ShingHei Kwok for their contribution in editing the paper.

Conflicts of Interest: The authors declare no conflict of interest.

References

1. Tran, M.-K.; Bhatti, A.; Vrolyk, R.; Wong, D.; Panchal, S.; Fowler, M.; Fraser, R. A Review of Range Extenders in Battery Electric Vehicles: Current Progress and Future Perspectives. *World Electr. Veh. J.* **2021**, *12*, 54. [\[CrossRef\]](#)
2. Shamsi, H.; Tran, M.-K.; Akbarpour, S.; Maroufmashat, A.; Fowler, M. Macro-Level Optimization of Hydrogen Infrastructure and Supply Chain for Zero-Emission Vehicles on a Canadian Corridor. *J. Clean. Prod.* **2020**, *289*, 125163. [\[CrossRef\]](#)
3. Amrouche, S.O.; Rekioua, D.; Rekioua, T. Overview of Energy Storage in Renewable Energy Systems. *Int. J. Hydrogen Energy* **2015**, *41*, 20914–20927. [\[CrossRef\]](#)
4. Tran, M.; Panchal, S.; Chauhan, V.; Brahmabhatt, N.; Mevawalla, A.; Fraser, R.; Fowler, M. Python-Based Scikit-Learn Machine Learning Models for Thermal and Electrical Performance Prediction of High-Capacity Lithium-Ion Battery. *Int. J. Energy Res.* **2021**, 1–9. [\[CrossRef\]](#)
5. Xie, J.; Lu, Y.-C. A Retrospective on Lithium-Ion Batteries. *Nat. Commun.* **2020**, *11*, 2499. [\[CrossRef\]](#)
6. Tran, M.-K.; Sherman, S.; Samadani, E.; Vrolyk, R.; Wong, D.; Lowery, M.; Fowler, M. Environmental and Economic Benefits of a Battery Electric Vehicle Powertrain with a Zinc-Air Range Extender in the Transition to Electric Vehicles. *Vehicles* **2020**, *2*, 398–412. [\[CrossRef\]](#)
7. Barcellona, S.; Piegari, L. Effect of Current on Cycle Aging of Lithium Ion Batteries. *J. Energy Storage* **2020**, *29*, 101310. [\[CrossRef\]](#)
8. Tran, M.-K.; Fowler, M. Sensor Fault Detection and Isolation for Degrading Lithium-Ion Batteries in Electric Vehicles Using Parameter Estimation with Recursive Least Squares. *Batteries* **2019**, *6*, 1. [\[CrossRef\]](#)
9. Tran, M.-K.; Fowler, M. A Review of Lithium-Ion Battery Fault Diagnostic Algorithms: Current Progress and Future Challenges. *Algorithms* **2020**, *13*, 62. [\[CrossRef\]](#)
10. Tran, M.-K.; Akinsanya, M.; Panchal, S.; Fraser, R.; Fowler, M. Design of a Hybrid Electric Vehicle Powertrain for Performance Optimization Considering Various Powertrain Components and Configurations. *Vehicles* **2020**, *3*, 20–32. [\[CrossRef\]](#)
11. Dubarry, M.; Vuillaume, N.; Liaw, B.Y. From Single Cell Model to Battery Pack Simulation for Li-Ion Batteries. *J. Power Sources* **2009**, *186*, 500–507. [\[CrossRef\]](#)
12. Zhou, L.; Zheng, Y.; Ouyang, M.; Lu, L. A Study on Parameter Variation Effects on Battery Packs for Electric Vehicles. *J. Power Sources* **2017**, *364*, 242–252. [\[CrossRef\]](#)
13. Rogers, D.J.; Aslett, L.J.; Troffaes, M.C. Modelling of Modular Battery Systems under Cell Capacity Variation and Degradation. *Appl. Energy* **2020**, *283*, 116360. [\[CrossRef\]](#)
14. Winslow, K.M.; Laux, S.J.; Townsend, T.G. A Review on the Growing Concern and Potential Management Strategies of Waste Lithium-Ion Batteries. *Resour. Conserv. Recycl.* **2018**, *129*, 263–277. [\[CrossRef\]](#)
15. Hossain, E.; Murtaugh, D.; Mody, J.; Faruque, H.M.R.; Sunny, S.H.; Mohammad, N. A Comprehensive Review on Second-Life Batteries: Current State, Manufacturing Considerations, Applications, Impacts, Barriers & Potential Solutions, Business Strategies, and Policies. *IEEE Access* **2019**, *7*, 73215–73252. [\[CrossRef\]](#)
16. Peterson, S.B.; Whitacre, J.; Apt, J. The Economics of Using Plug-in Hybrid Electric Vehicle Battery Packs for Grid Storage. *J. Power Sources* **2010**, *195*, 2377–2384. [\[CrossRef\]](#)
17. Foster, M.; Isely, P.; Standridge, C.R.; Hasan, M. Feasibility Assessment of Remanufacturing, Repurposing, and Recycling of End of Vehicle Application Lithium-Ion Batteries. *J. Ind. Eng. Manag.* **2014**, *7*, 698–715. [\[CrossRef\]](#)
18. Kampker, A.; Wessel, S.; Fiedler, F.; Maltoni, F. Battery Pack Remanufacturing Process up to Cell Level with Sorting and Repurposing of Battery Cells. *J. Remanufacturing* **2020**, *11*, 1–23. [\[CrossRef\]](#)
19. Mathew, M.; Kong, Q.; McGrory, J.; Fowler, M. Simulation of Lithium Ion Battery Replacement in a Battery Pack for Application in Electric Vehicles. *J. Power Sources* **2017**, *349*, 94–104. [\[CrossRef\]](#)
20. Nenadic, N.G.; Trabold, T.A.; Thurston, M.G. Cell Replacement Strategies for Lithium Ion Battery Packs. *Batteries* **2020**, *6*, 39. [\[CrossRef\]](#)
21. Lu, Y.; Li, K.; Han, X.; Feng, X.; Chu, Z.; Lu, L.; Huang, P.; Zhang, Z.; Zhang, Y.; Yin, F.; et al. A Method of Cell-to-Cell Variation Evaluation for Battery Packs in Electric Vehicles with Charging Cloud Data. *eTransportation* **2020**, *6*, 100077. [\[CrossRef\]](#)
22. Omariba, Z.B.; Zhang, L.; Sun, D. Review of Battery Cell Balancing Methodologies for Optimizing Battery Pack Performance in Electric Vehicles. *IEEE Access* **2019**, *7*, 129335–129352. [\[CrossRef\]](#)
23. Rehman, M.M.U.; Zhang, F.; Evzelman, M.; Zane, R.; Smith, K.; Maksimovic, D. Advanced Cell-Level Control for Extending Electric Vehicle Battery Pack Lifetime. In Proceedings of the 2016 IEEE Energy Conversion Congress and Exposition (ECCE), Milwaukee, WI, USA, 18–22 September 2016; pp. 1–8. [\[CrossRef\]](#)
24. Zheng, Y.; Ouyang, M.; Lu, L.; Li, J. Understanding Aging Mechanisms in Lithium-Ion Battery Packs: From Cell Capacity Loss to Pack Capacity Evolution. *J. Power Sources* **2015**, *278*, 287–295. [\[CrossRef\]](#)
25. Belt, J. Battery Test Manual for Plug-In Hybrid Electric Vehicles. *Tech. Rep.* **2010**. [\[CrossRef\]](#)
26. Tran, M.-K.; Mevawala, A.; Panchal, S.; Raahemifar, K.; Fowler, M.; Fraser, R. Effect of Integrating the Hysteresis Component to the Equivalent Circuit Model of Lithium-Ion Battery for Dynamic and Non-Dynamic Applications. *J. Energy Storage* **2020**, *32*, 101785. [\[CrossRef\]](#)
27. Tran, M.-K.; DaCosta, A.; Mevawalla, A.; Panchal, S.; Fowler, M. Comparative Study of Equivalent Circuit Models Performance in Four Common Lithium-Ion Batteries: LFP, NMC, LMO, NCA. *Batteries* **2021**, *7*, 51. [\[CrossRef\]](#)

28. Tran, M.-K.; Mathew, M.; Janhunen, S.; Panchal, S.; Raahemifar, K.; Fraser, R.; Fowler, M. A Comprehensive Equivalent Circuit Model for Lithium-Ion Batteries, Incorporating the Effects of State of Health, State of Charge, and Temperature on Model Parameters. *J. Energy Storage* **2021**, *43*, 103252. [[CrossRef](#)]
29. Hu, X.; Li, S.; Peng, H. A comparative study of equivalent circuit models for Li-ion batteries. *J. Power Sources* **2012**, *198*, 359–367. [[CrossRef](#)]
30. Deng, Z.; Hu, X.; Lin, X.; Xu, L.; Che, Y.; Hu, L. General Discharge Voltage Information Enabled Health Evaluation for Lithium-Ion Batteries. *IEEE/ASME Trans. Mechatron.* **2020**, *26*, 1295–1306. [[CrossRef](#)]
31. Hu, X.; Yuan, H.; Zou, C.; Li, Z.; Zhang, L. Co-Estimation of State of Charge and State of Health for Lithium-Ion Batteries Based on Fractional-Order Calculus. *IEEE Trans. Veh. Technol.* **2018**, *67*, 10319–10329. [[CrossRef](#)]
32. Schmalstieg, J.; Käbitz, S.; Ecker, M.; Sauer, D.U. A Holistic Aging Model for Li(NiMnCo)O₂ Based 18,650 Lithium-Ion batteries. *J. Power Sources* **2014**, *257*, 325–334. [[CrossRef](#)]
33. Ng, K.S.; Moo, C.-S.; Chen, Y.-P.; Hsieh, Y.-C. Enhanced Coulomb Counting Method for Estimating State-of-Charge and State-of-Health of Lithium-Ion Batteries. *Appl. Energy* **2009**, *86*, 1506–1511. [[CrossRef](#)]
34. Gabbar, H.; Othman, A.; Abdussami, M. Review of Battery Management Systems (BMS) Development and Industrial Standards. *Technologies* **2021**, *9*, 28. [[CrossRef](#)]
35. Beard, K.W.; Reddy, T.B. *Linden's Handbook of Batteries*, 5th ed.; McGraw-Hill: New York, NY, USA, 2019; ISBN 978-1-260-11592-5.
36. Lee, S.S.; Kim, T.H.; Hu, S.J.; Cai, W.W.; Abell, J.A. Joining Technologies for Automotive Lithium-Ion Battery Manufacturing: A Review. In Proceedings of the ASME 2010 International Manufacturing Science and Engineering Conference, Erie, PA, USA, 12–15 October 2010; Volume 1, pp. 541–549. [[CrossRef](#)]
37. Wentker, M.; Greenwood, M.; Leker, J.; Wentker, M.; Greenwood, M.; Leker, J. A Bottom-Up Approach to Lithium-Ion Battery Cost Modeling with a Focus on Cathode Active Materials. *Energies* **2019**, *12*, 504. [[CrossRef](#)]